5G mmWave Network Planning Using Machine Learning for Path Loss Estimation

YOSVANY HERVIS SANTANA [1,2], RODNEY MARTINEZ ALONSO [1,3] (Senior Member, IEEE),
GLAUCO GUILLEN NIETO[2] (Senior Member, IEEE), LUC MARTENS [1] (Member, IEEE),
WOUT JOSEPH [1] (Senior Member, IEEE), AND DAVID PLETS [1] (Member, IEEE)

[1]Department of Information Technology, IMEC, Ghent University, 9052 Ghent, Belgium

[2]Research and Development Telecommunications Institute, LACETEL, Havana 19210, Cuba

[3]Department of Electrical Engineering, KU Leuven, 3000 Leuven, Belgium

CORRESPONDING AUTHOR: Y. H. SANTANA (e-mail: yosvany.hervissantana@ugent.be)

ABSTRACT New frequency bands, such as the mmWave at 28 GHz for fifth Generation networks in Frequency Range 2, are being introduced to accomplish the required throughput for new services such as remote surveillance, object tracking, and factory automation. These high-frequency bands are sensible to reflections and diffraction. Therefore, accurate path loss calculation relies on advanced models and ray tracing. However, this is time-consuming, and evaluating a large set of candidate solutions is no longer possible when planning the optimal number and location of base stations in the network planning process. This paper investigates the use of machine learning to approximate a complex mmWave ray-tracing-based path loss model in indoor scenarios. The much lower calculation time allows us to approximate the ray-tracer path loss estimation well and to apply a genetic algorithm for realizing network planning. The machine learning model is trained and validated for two buildings and tested with another, with an average of the Mean Absolute Error of 2.8 dB over all cases. It is shown that the combination of Machine Learning and Genetic Algorithm is able to find a network deployment in the FR2 band accounting for the minimum number of access points and minimum electromagnetic exposure, while still providing a predefined coverage percentage inside the building.

INDEX TERMS 28 GHz, 5G, FR2, genetic algorithm, network planning, mmWaves, modeling machine learning, path loss, ray tracing, wireless InSite.

I. INTRODUCTION

FIFTH-GENERATION (5G) Technology is designed to broaden the reach of mobile technology beyond Long-Term Evolution (LTE) capabilities [1]. The 5G mobile initiative is a tremendous collective effort to specify, standardize, design, manufacture, and deploy the next cellular network generation. 5G is characterized by three key features: faster speeds, lower latency, and the ability to connect many devices at the same time [2]. It will support demanding services such as enhanced Mobile Broadband, Ultra-Reliable, Low Latency Communications, and massive Machine-Type Communications, which will require high data rates and latencies of a few milliseconds [3]. Because of higher bandwidth and new antenna technology, 5G enables a significant increase in data-rate sent through wireless systems [4]. It operates in two Frequency Ranges (FR): FR1 (includes sub-6 GHz), and FR2 (which includes the millimeter-wave band, from 24.25 to 52.6 GHz) [5].

Many of the use cases for 5G target indoor scenarios, among others, smart building monitoring, factory automation, and objects/people tracking inside a building/factory [6]. The easiest way to address these scenarios is via the existing outdoor network [7] but often, high building penetration losses impact the desired performance [8], [9]. In [8], the authors experimentally demonstrated a 30 dB - 100 dB (depending on the wall materials) excess path loss at distances beyond 50 m from the Base Station (BS). Hence,

understanding propagation characteristics in indoor scenarios is of vital importance in 5G networks.

Wireless network planning and optimizations play an important role in modern wireless communications. Usually, to find the optimal network deployment the evaluation of many candidate solutions is needed to meet requirements related to a targeted QoS and a minimal deployment cost, energy consumption, and/or human exposure. In indoor scenarios, the PL estimation is challenging because of the complexity of the environment and the impact of multipath. One option is to use heuristic models [10] or models based on ray-tracing (RT) techniques [11].

Especially at high frequencies (mmWave communications), reflections and diffractions are very sensitive to variations in the indoor propagation environment [12]. To estimate the Path Loss (PL) in these indoor environments a PL calculation based on ray-tracing (RT) models is more accurate than the use of traditional statistical models [13], [14]. However, RT models are much more time-consuming. When performing network planning, hundreds of candidate network deployments are evaluate [15]. Therefore, ray-tracing path loss models are less suited to use in the optimal network design process, as calculation time can become excessively or unfeasibly large.

In this research work, we propose a generic method based on the Gaussian Process (GP) algorithm for the PL estimation of 5G signals at 28 GHz in indoor environments. The obtained model is much quicker to evaluate and is used in combination with a Genetic Algorithm (GA) [16] to perform 5G network planning, allowing finding an optimal network deployment, which would not be possible using a ray tracing-based path loss model. The novelty of this research article is (i) we propose a generic machine learning model that can approximate Path Loss (PL) in indoor environments for mmWaves, (ii) we demonstrate the effectiveness of combining ML + GA for wireless network planning, which can lead to more efficient and optimized network deployments, (iii) we perform network deployment that ensures a minimum coverage percentage (95-100%) and accounts for minimum Human Electromagnetic Exposure based on the ray-tracing PL model, and (iv) we present a flexible solution that can quickly optimize deployments with other Quality of Service (QoS), energy, and/or exposure constraints, performing a Pareto analysis.

We show that an advanced and computationally expensive path loss model, like the one based on RT methods, can be well approximated by a ML-based PL model, allowing faster PL calculation for a given area. Such a quick, but still accurate PL model allows the possibility of more thorough exploration of the optimization space to find the optimal network deployment (number and location of APs). It is shown that the proposed approach is accurate and able to meet flexible coverage requirements (95% to 100%) and allows easy replanning with adjusted optimization settings,

thanks to the largely reduced time to explore the solution space.

The remainder of this paper is organized as follows. Section II discusses related works on mmWave PL estimation and network optimization approaches in the mmWave band. Section III describes the scenarios for designing the model, and the method used to estimate the PL. Section IV discusses the performance of the PL estimation using the ML algorithm. Also, we investigate the quality of the resulting network planning solution, by comparing it with the Remcom Wireless InSite software (RT-based tool) output in terms of the coverage percentage of the ML-GA-based network design. Finally, Section V presents the conclusions of this research.

II. RELATED WORKS
A. PATH LOSS ESTIMATION AND MACHINE LEARNING (ML)

In [17], the authors investigated several simple machine learning models like an Artificial Neural Network (ANN) or Linear Regression Model to predict the received signal strength in wireless networks (WIFI, 2.4 GHz) based on environmental parameters, with the best performance in terms of Mean Squared Error (MSE) and Mean Absolute Error (MAE = 4.92 dB for the training dataset and MAE = 5.37 dB for the testing dataset) achieved for the ANN model. The main limitation of this research is related to constructing the dataset and building the ML model. The authors used a fixed AP position for building the dataset, which limits the generality and affects the performance of the ML model if the AP is moved to another location with more obstacles. In [18], the authors proposed a deep learning-based indoor WiFi (5 GHz) path loss modeling approach, specifically, an algorithm that generates input images based on measurement locations and a floor plan. The input images contain information regarding the propagation environment between the fixed access points (AP) and measurement locations. A convolutional neural network (CNN) model was trained to learn the features of the indoor environment and approximate the underlying functions of the WiFi signal propagation. Its deep learning-based indoor path loss model was shown to achieve superior performance over 3D ray-tracing methods. The average root mean square error (RMSE) between the predicted and measured received signal strength values in the two scenarios was 4.63 dB. The universality of this model is limited though, as using the model in a new scenario requires training the ML model with information related to the new building/office/house. In [19], a new training strategy to train PL models at 28 GHz band based on a convolutional neural network (CNN) was proposed. The strategy was based on meta-learning which performs well in few-shot learning scenarios with multiple tasks comprising a meta-task. It was shown that the indoor PL model based on a CNN configured with multiple beams can outperform the CNN models by a conventional training algorithm as well as empirical models.

The authors mentioned that the model could be applied in other scenarios, but no results were shown regarding this statement. In [20], the authors reported the inclusion of Kriging as a tool for modeling mmWave indoor propagation, as it considers all the singularities and site-associated features that are implicit in the measured samples. For the 28 GHz band, the Kriging-aided model improves the accuracy in predicting path loss with 3.1 dB RMSE (3.6 dB RMSE without the Kriging model). In this study, the authors did not provide details about the dataset construction and the inputs used to train the ML algorithm, which makes it difficult to know the generacity of the model. In addition, they did not provide details related to the time required to perform calculations. In [21], the authors presented a methodology of data-driven techniques applied to predict path loss in 28 GHz using ML algorithms (random forest, decision tree, lasso regression, gradient boosting, and neural network-deep learning). The data for building the dataset was described in [22] and updated in this research to reflect an indoor environment. The authors compared the estimation performance of all the five proposed algorithms with measurement results, at the 28-GHz band, and the highest R^2 accuracy of 97.4% was achieved by the random forest algorithm. In this study, the authors did not provide information about the geography of the scenario, the number of walls, and the wall material. In addition, all the inputs for the ML model (at least the ones stated in the manuscript) are not related to the environment, which might affect the model's performance in case of using it in other indoor scenarios. In [23], the authors introduced a deep learning model (U-Net architectures) that estimates simulated indoor radio propagation maps at 5 GHz. To generate the dataset, the authors avoid proprietary software because they require manual inputs of floor plans and simulation parameters, which is not feasible when simulating hundreds or thousands of scenarios. The inputs are white and black floor plans describing the walls in the scenarios and up to five AP positions. The authors obtained an MAE of around 1 dB in a small portion of 20 x 20 m2 in a university building. The proposed method was at least 30 times faster than WinProp software. However, the paper lacks a validation in another building. Also, they did not use the model for network deployment optimization. In [24], the authors introduced a Python-based tool designed to enhance the prediction of wireless network signals for WIFI 2.4 GHz and 5Ghz in indoor settings using neural networks. The approach employed allows for adaptive learning from the environment to improve prediction accuracy. By comparing with real measurements, the study demonstrated its superior accuracy (MAE = 3.5 dB) in signal loss prediction against traditional models (best performance for One Slope model with MAE = 19.4 dB) through comparative analysis. Despite the results, the authors limited their comparison only to the traditional models. In larger environments, with a higher number of obstacles, the universality of the tool could be compromised.

B. PATH LOSS ESTIMATION USING RAY-TRACING METHODS

Several works have tried to emulate the signal propagation in indoor and outdoor environments [13], [15], [25], [26]. At higher frequencies, ray-tracing approaches have shown to be more accurate in predicting PL [27], but the required time and computer power needed make it difficult to perform several simulations and achieve good accuracy. In [15], the authors conducted a ray-tracing simulation using a 3D floor plan. The obtained results show that the existing indoor solutions operating at 2.6 GHz can be reused at 3.5 GHz frequency with minor power adjustment, or by using antennas with a little higher gain. However, the authors stated that a new deployment (the existing one does not meet the coverage requirements) is required due to the complexity of the environment for an Ultra Dense Network at 28 GHz. In [25], the authors developed an Adaptive Path Sensing Method (APSM) for indoor radio wave propagation prediction at 4.5 GHz, 28 GHz, and 38 GHz. Measurement campaigns, which cover indoor line-of-sight (LOS), non-line-of-sight (NLOS), and different room scenarios were conducted. The proposed method was evaluated through a computerized modeling tool by comparing the Received Signal Strength Indicator (RSSI) with measurement data and the conventional Shooting-Bouncing Ray-Tracing (SBRT) method. The experiment was conducted with one transmitter and 83 receivers in an in-house scenario with 21 m x 30 m. The simulations were performed for one receiver each time (after all the rays are launched the Rx point was re-positioned). The needed time for launching all the rays for one Rx was around 7 seconds. The comparison results show that the APSM achieves higher RSSI accuracy than SBRT and takes 7 seconds for the combination Tx-Rx vs. 23 seconds for the SBRT method (the process was repeated 83 times, one time per Rx point). The proposed APSM method has effectively minimized the computational resources and time needed by 60%. However, to perform network planning (evaluation of hundreds of AP candidates), with a higher number of Rx points the required time is too high. In [26], the authors developed and experimentally validated an Efficient Three-Dimensional Ray-Tracing (ETRT) method to calculate the indoor radio wave propagation at 28 GHz. Compared with the conventional SBRT method, the proposed ETRT method showed better agreement with measurement data. Despite the accuracy achieved in this research, the authors do not mention any improvement in the required calculation time and the needed computational power. In [13], the authors proposed a simplification that can reduce the complexity of the ray-tracing in the mmWave without significantly affecting the model's accuracy. Specifically, they considered processing only multipath components (MPCs) whose received power is above a certain threshold, relative to the strongest MPC, and limiting the maximum number of reflections for each MPC. They demonstrated that by limiting the MPC the complexity and calculation time were reduced from hundreds of minutes to hundreds of seconds.

The research works stated in this section demonstrate that the ray-tracing method offers good accuracy in terms of propagation path loss calculation at mmWave frequencies, but is time-consuming. Many efforts have been conducted to simplify the algorithms together with the required time to make calculations. To accomplish the objective, the authors used a reduced number of transmitters and receivers in the scenarios. However, to use those results in a realistic situation and perform network design, hundreds of AP candidates should be evaluated for providing coverage to a floor. In these cases, the required time to calculate one network deployment plays an important role. The research in this work is focused on a method based on ML (to estimate the PL) and GA (to find the optimal AP distribution on a floor) using the ML PL model, to find network designs subject to constraints (coverage, cost, and human exposure).

C. ELECTROMAGNETIC HUMAN EXPOSURE

The increasing use of wireless networks in our life has generated a common concern related to the general public's exposure to RF (radio-frequency) electromagnetic fields used for wireless telecommunication. International Institutions such as IEEE [28] and ICNIRP (International Commission on Non-Ionizing Radiation Protection) [29] have issued safety guidelines to limit the maximal electric-field strength due to wireless communications. A lot of research has been conducted on the characterization of RF exposure [30], [31], [32].

In [30], the authors developed a heuristic indoor network planner for exposure calculation and optimization of wireless networks, jointly optimizing coverage and exposure, for homogeneous WiFi or heterogeneous networks (WiFi-LTE). In [31], the authors minimized the whole-body exposure doses (uplink and downlink) for indoor wireless network deployments in four simulation scenarios. For WiFi, downlink doses were reduced by more than 95% by the optimized deployment and for UMTS, total dose reductions varied between 73% and 83%. In [32], the authors designed a multi-objective optimization algorithm implemented to maximize the user coverage while minimizing the downlink (DL) and uplink (UL) exposure in a 5G network topology.

D. NETWORK OPTIMIZATION AT MMWAVE FREQUENCIES

5G networks are also being deployed over mmWave (28 GHz) where ray-tracing models have been shown to perform well to estimate the PL. In [33], an attempt has been made to perform network planning using an RT-based PL model. The authors proposed an algorithm for determining the minimum number of transmitting antennas as well as their appropriate locations to provide optimized wireless coverage in the indoor environment. The proposed algorithm uses a ray-tracing method to estimate the received signal level among 6 sampling points in the indoor area due to one or more transmitters and the Genetic Algorithm (GA) incorporated with the Breadth First Search (BFS)

to determine the minimum number of transmitters and their corresponding locations to achieve the optimum wireless coverage. The algorithm achieved better performance compared with existing ones, reducing the computation time by as much as 99%. However, to perform network evaluations the authors only evaluated 6 AP candidates with a maximum of 25 receiver points. In [34], the authors aimed to optimize the deployment of indoor small base stations (5G at 3.5 GHz) using a hybrid algorithm that combines differential evolution and particle swarm optimization (PSO). The core methodology involves correcting the wireless propagation model ITU R.P. 1238 using the least squares method to account for real-world nonlinearities that affect signal propagation indoors. The authors concluded that the method provides a robust solution for indoor wireless network layout planning. Despite the assessment, this approach was tested in a room of 15x15x3 m and with a very simple floor plan. To prove the generality of the model the authors did not provide any evidence of the performance in a more complex room/floor.

Most PL models at higher (e.g., 28 GHz) frequencies are RT-based. To the authors' knowledge, no more 5G network planning at 28 GHz (or at mmWave frequencies) has been executed due to the large RT calculation time, making a thorough exploration of the solution space impossible. No attempts (to the best of our knowledge) have been made yet to optimize (downlink (DL)) exposure due to indoor 5G network deployments. This research will aim at mimicking a 28 GHz RT-based PL with machine learning to offer a flexible 5G network deployment optimization tool at 28 GHz, able to account for coverage and exposure requirements.

III. METHODS AND SCENARIOS

This section describes the indoor network planning methodology, using a machine-learning generated path loss model obtained from ray tracing simulations, incorporated into a genetic algorithm for finding the optimal network deployment (number and location of 5G stations at 28 GHz). First, for a large set of transmit-receive links in a set of training buildings, we use a ray-tracing tool to calculate the target PL [dB]. For each of these links, we also determine a set of easy-to-calculate inputs (minimizing calculation time but expecting to have a large predictive power for the path loss, see Table 2). With this set of inputs and with the target PL from the ray-tracing tool as output, we train and validate (this process is only executed once until we obtain the trained model) a Machine Learning model that approximates the ray-tracing PL, but is calculated much faster. In a second stage, we rely on the estimated PL from the created ML model (see Section II-E.3) in a Genetic Algorithm that searches for an optimal wireless network deployment, subject to coverage constraints (at least the 95% of all possible Rx points must be covered) and striving for a minimum number of deployed base stations, and minimum electromagnetic exposure. This ML model is a less complex approximation
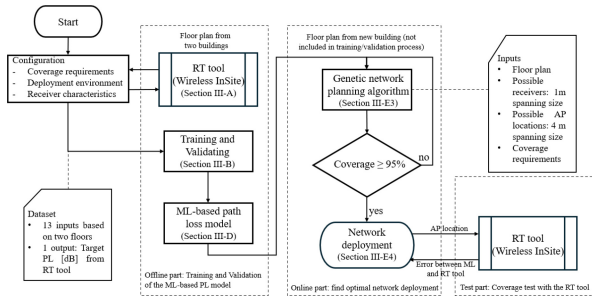
FIGURE 1. Flow-graph of the proposed approach and its validation with the Wireless InSite. RT: ray-tracing; ML: Machine Learning.

of the ray-tracing PL model. Consequently, the model can be used in a GA, which requires the evaluation of a lot of candidate deployment solutions, and thus, a lot of otherwise time-consuming path loss calculations. For the purpose of validating our proposed approach, the received power and coverage percentage of the deployments obtained with the ML-based path loss model in the area compared with the results obtained using the initial ray tracer path loss model. Figure 1 shows a flow graph of the proposed approach.

Compared to the typical log-distance, multi-wall model, or Indoor Dominant Path (IDP) model based on [10], the RT method for PL models is more advanced, as it evaluates the different paths between transmitter and receiver. The goal of the ML model is to accurately estimate this PL value, based on a set of relevant inputs that can be easily obtained or calculated. In our research, an ML algorithm is trained and validated with input variables that have a low calculation time, such as the distance between the AP and the receiver locations, the number of walls in the direct line to the source, and wall penetration loss. To calculate the losses related to the walls we consider the incident angle of the direct beam from Tx to Rx and the materials of the walls. To account for the impact of reflecting walls, we include reflection losses of rays under four NLoS directions (± 10°/20° with respect to the LoS direction). Finally, to assess the ML model performance, we compare the PL estimated with the ML and the PL calculated with the Wireless InSite software [35], [36].

A. REMCOM WIRELESS INSITE FOR PATH LOSS GENERATION

The 3D RT method used was executed via Remcom Wireless InSite 3.3.5 software. We used the X3D variant of the ray-tracing method, which supports efficient parallel computations using multi-core Compute Unified Device Architecture (CUDA)- capable Graphics Processing Units (GPUs), and a processor, such as the Nvidia GForce RTX 3050Ti series.

The X3D ray model was developed by Remcom to provide a highly accurate, full 3D propagation model capable of running on a graphics processing unit (GPU) and using multi-threading for fast runtimes. This model also uses Remcom's depth-first and exact path algorithms to overcome some of

the shortcomings of the traditional SBRT. X3D does not have any restrictions on geometry shape or transmitter/receiver height. This accurate model includes reflections, transmissions and diffractions, and frequency-dependent atmospheric absorption. The SBRT method requires a collection radius to be constructed around receiver locations to compensate for the discrete ray shooting. Any rays intersecting the sphere are considered to reach the receiver. The exact path corrects SBR ray paths so that they end at the exact receiver location. This correction reduces errors in calculated power and phase associated with SBR but at the cost of longer run times required by methods based on image theory [35], [36], [37].

B. PATH LOSS ESTIMATION USING MACHINE LEARNING

In the Wireless InSite software, the needed time for calculating the received signal in all the grid points (1107 points located with a grid size of 1 m, see Figure 2(e)) for one AP is around 2 minutes for the 5th floor of the iGent building. Therefore, we investigate if these advanced PL models can be well approximated using an ML model. We here apply the Gaussian Process (GP) for regression [38], [39]. Regression models based on GP are simple to implement, flexible, and fully probabilistic models [39]. The ML will estimate the PL (i.e., dependent variable, model output) using equation (2) after being fed with a number of inputs (i.e., independent variables) that have a correlation with the output variable. To achieve the desired accuracy, the algorithm must be trained and validated to learn which is the output that corresponds to the given inputs using a training dataset (known samples where a number of inputs corresponding to a true output). During the training process, the ML model iteratively adjusts its coefficients to minimize the MAE between the predicted and the true path loss using Equation (1), where N is the number of observations in the training and validation dataset, PL_{ML} is the PL estimation made by the ML model using a vector of inputs, and PL_{WI} is the PL calculated by the RT software, for observation i.

$$MAE = \frac{1}{N} \sum_{i=1}^{N} |PL_{ML} - PL_{WI}| \qquad (1)$$

1) GAUSSIAN PROCESS ALGORITHM

Gaussian Processes (GPs) are an approach to regression problems. This section aims to present the basics of GPs without going too deep into the algorithm. For a more elaborate discussion of GPs, we refer the reader to more detailed literature [40]. The prediction problem can be formulated as follows: given a set of N observations $Y = \{y_1, y_2, \ldots, y_N\}$ of a dependent variable (PL values) and the independent variables would be the vector $X = \{x_1, x_2, \ldots, x_N\}$ in the Gaussian Process framework where $x_1, x_2, \ldots, x_N$ each are 13-dimensional input vectors (see Table 2, Section III-D). By dividing the dataset in n samples for training and m samples for validating the model (where $N = n + m$) the X and Y vectors can be defined as, $Y =$
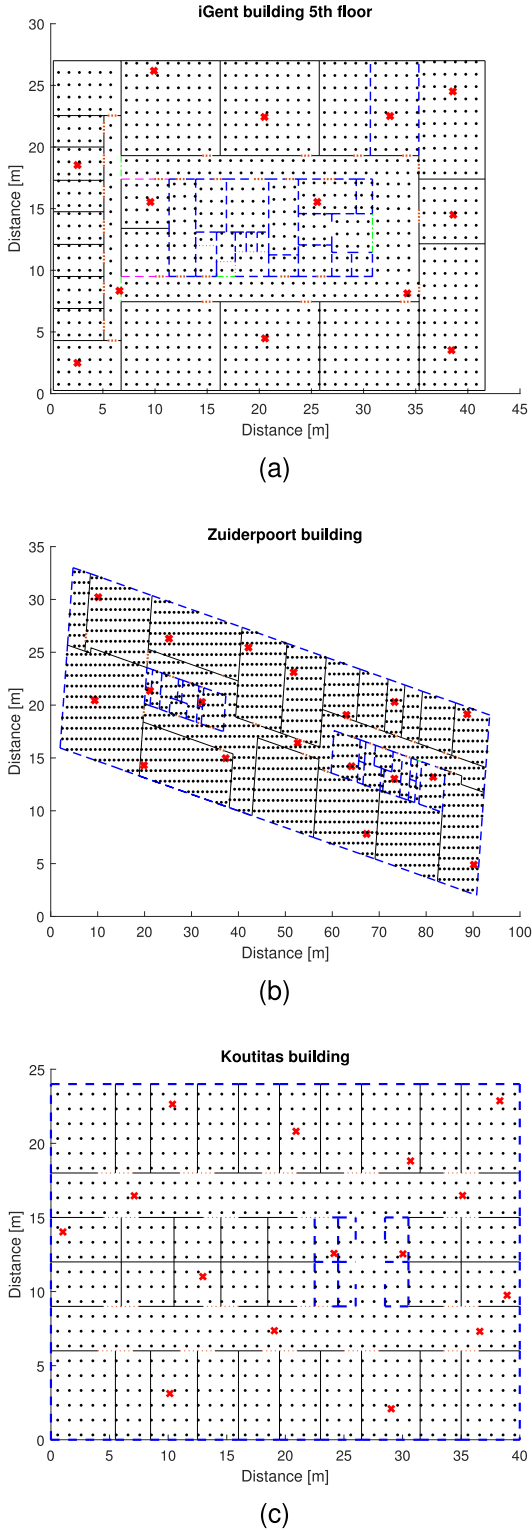
FIGURE 2. Indoor environments with APs locations used to generate the training and validation datasets. Red crosses represent the APs locations. Black dots represent the Rx points with a grid size of 1 m. (a) iGent building 5thth floor (b) Zuiderpoort building 3rd floor (c) Koutitas building.

$\{y_1, y_2, \ldots, y_n\}$ and $X = \{x_1, x_2, \ldots, x_n\}$ as training vectors, and $Y_* = \{y_1, y_2, \ldots, y_m\}$ and $X_* = \{x_1, x_2, \ldots, x_m\}$ as validation vectors.

Consider an observation y (see Equation (2)), which can be described by the kernel function or covariance function of the Gaussian process distribution [40]. The kernel function together with the mean function f(X) define the Gaussian process distribution.

$$Y \sim GP(f(X), K(X, X)) \qquad (2)$$

The objective is now to predict the Y_* (PL_{ML} in equation (1)) given the validation input X_*. Recalling that a GP is a set of variables which have a consistent Gaussian distribution with mean zero, we can represent our problem as equation (3) [41]:

$$\begin{bmatrix} f \\ f_* \end{bmatrix} \sim N\left(0, \begin{bmatrix} K(X, X) + \sigma_n^2 I & K(X, X_*) \\ K(X_*, X) & K(X_*, X_*) \end{bmatrix}\right) \qquad (3)$$

Here, $\sigma_n^2 I$ is distributed noise added to the Gaussian process distribution with variance σ_n. $K(X, X_*)$ provides the covariance between the training values (X) and the validation values (X_*) whose output value (Y_*) we are estimating. $K(X_*, X_*)$ represents the similarity of any two observations from the vector X_*.

Once defined the problem, it is straightforward to make predictions for new test points, using straightforward algebraic matrix manipulation. However, in practical applications it is unlikely to know which covariance function to use. The exponentiated quadratic kernel (also known as squared exponential kernel, Gaussian kernel or radial basis function kernel) is a popular kernel used in Gaussian process modeling and can be computed as:

$$K(X, X_*) = \sigma_f^2 exp\left(-\frac{1}{2l^2}(X - X_*)^2\right) + \sigma_m^2 \delta \qquad (4)$$

The reliability of our regression is then dependent on how well we select the parameters that the selected covariance function requires (l, σ_f, σ_m) [42]. Assume $\Theta = \{l, \sigma_f, \sigma_m\}$ as a set of hyperparameters needed for a given covariance function, where l is the length-scale (corresponds to the frequency of the functions represented by the Gaussian process), σ_f the signal noise and σ_m the noise variance. Because of its simplicity, in this work we use the Gradient Descent technique to find the set of near-optimal hyperparameters in equation (4).

C. STUDY AREAS

For training and validating, and testing our model we investigate three different buildings (iGent and Zuiderpoort in Ghent, Belgium, and the building used in Koutitas and Samaras [43], further denoted as 'Koutitas', Table 1) with different characteristics and complexity. To obtain a general model, we selected buildings with different layouts and types of walls (materials and thickness) and penetration losses. To build the model, we train and validate with the information from two buildings and test it with the third one (not in the training and validating dataset). This process is repeated for all three possible combinations.

TABLE 1. iGent and Zuiderpoort are office buildings in the city of Ghent, Belgium, and Koutitas, in Greece. AP = Access Point.

Building	Area [m²]	# 5G Sources (AP)	Total Number of PL samples
iGent (5th floor)	42 x 27	13	14391
Zuiderpoort (3rd floor)	82 x 17	18	27234
Koutitas	40 x 24	15	14400

The investigated buildings are described in Table 1. The aim is to deploy 5G sources operating at 28 GHz, placed at 2.5 m above the ground, with an Equivalent Isotopically Radiated Power (EIRP) configurable between 5 dBm and 40 dBm. The 5G receiver was assumed to be at carrying height, i.e., 1.3 m, above the ground level.

A general RT procedure relies on a ray-optics approximation of the Maxwell equations. A transmitter is modeled by launching rays from its center in a finite set of directions, distributed over the complete unit sphere. A ray is propagated through the environment predefined with its geometry and material properties, undergoing reflections, refractions, and diffractions, until its power reaches a predefined threshold. If a ray passes in the vicinity of a receiver, it contributes to the total field at that receiver's location. Assuming that terminals (or points of interest) can be distributed all around 360 degrees around AP, with the purpose of accounting for the maximum possible level at any point, the AP will be treated (also the receivers) as having an equivalent omnidirectional antenna with the gain equal 2.15 dB. To construct a training dataset we put several APs (13 APs for the iGent 5th floor, 18 for the Zuiderpoort building, and 15 for the Koutitas building, see Figure 2(e)) located at 2.5 m high, transmitting at 20 dBm. To build a model based on the building environment, it was necessary to consider the electromagnetic parameters of the walls and other structural elements, such as concrete walls, brick walls, and partition walls made of drywall. The electromagnetic parameters of all elements were extracted from the ITU documents [44], with the incidence angle, we calculate the reflection and penetration losses based on the Fresnel formulas for reflection and transmission [45].

D. DATASET CONSTRUCTION

For training, validating, and testing the ML PL model we analyze three buildings. We use RT simulation data from two buildings to train and validate the ML model and the third building is used for testing (not included in the training and validating process, see Section III-C). In the buildings used for training and validating the model, we include all information from all APs is in the same dataset to have a maximal of training PL samples. For evaluation of the ML PL model on the third building (test building), we consider 5 random AP locations: we estimate the path loss for all the AP-to-grid point links with the constructed ML model

and compare the result with the RT software-generated PL value. Each building is equipped with several 5G sources (Table 1), and the PL information is generated according to the Remcom Wireless InSite ray-tracing software. These PL samples are calculated on a 1 m regular grid spanning the entire building, between APs and receiver locations. The goal is to estimate the PL (output) samples, not by finding the different paths between Tx and Rx (like RT models), but based on a set of 13 easy-to-calculate inputs (See Table 2). These inputs are expected to have a predictive power for the path loss and are easy to calculate, minimizing calculation time for the ML model.

1) MAE VALIDATION AND NUMBER OF APS FOR MODEL TRAINING

To build the training dataset we simulate the PL between different AP locations and receiver locations in the building, using the ray-tracing software (Section III-A). To determine the minimum required number of APs to create the training dataset for one-specific building, we adopt the following procedure. The resulting dataset from the combination of AP-Rx links is denoted D_i, where i is the index of the simulated AP. Combining the information from different APs in a floor, we generate different sub-datasets $(D_1, D_2, D_3, \ldots, D_n$, where, n = total number of AP). For training, we increase the number of samples by adding a dataset D until the information from one dataset remains to validate the model (see steps below). However, in the validation process, we use a single dataset (D) and calculate its MAE. The final MAE of each step is the mean of all MAEs for every single D. To validate the MAE we use the following procedure:

- Train with $D = [D_1]$, validate with $D_2; D_3; \cdots; D_n$, and $MAE = Mean(MAE_{D_2}; MAE_{D_3}; \cdots; MAE_{D_n})$
- Train with $D = [D_1; D_2]$, validate with $D_3; D_4; \cdots; D_n$, and $MAE = Mean(MAE_{D_3}; MAE_{D_4}; \cdots; MAE_{D_n})$
- Train with $D = [D_1; D_2; D_3]$, validate with $D_4; D_5; \cdots; D_n$, and $MAE = Mean(MAE_{D_4}; MAE_{D_5}; \cdots; MAE_{D_n})$
- The process continues until $D = [D_1; D_2; \ldots; D_{n-1}]$ and validate with D_n.

Finally, to estimate the value of the MAE we calculate the Progressive Average (PAVE) of all previously calculated MAE values. If the MAE stabilizes, it means that the number of simulated APs is enough to train and validate the model. Otherwise, we need to calculate more PL values for different combinations of AP-Rx, where the AP location on the floor must be different.

E. NETWORK PLANNING AND GENETIC ALGORITHM

As no ray-tracing-based network planning output is available as a benchmark solution here, we evaluate the performance of the model in terms of the covered percentage. The GA-proposed solution is evaluated with the RT software and compared with our method to verify that in every Rx point, we meet the required quality of service.

TABLE 2. Description of the inputs used to build the dataset for training and validate the ML model.

Type	Description	Number of Elements
Inputs	log_{10} of the distance [m] between the 5G source and the given point [48]. PL (dB) generally decreases linearly with the logarithm of the distance	1
	Number of walls per type (glass, concrete, layered drywall, wood) along the ray Tx-Rx. Different wall materials cause different path attenuation.	4
	Total penetration loss along the direct ray. This is the sum of all penetration loss values along the ray Tx-Rx. Higher penetration loss along the direct ray is expected to lead to a higher path loss.	1
	Average penetration losses [dB] of all walls along the direct ray between the Tx to the Rx. It characterizes the attenuation to be expected in the building caused by the signal penetration.	1
	Average reflection losses [dB] of all walls along the direct ray between the Tx to the Rx. It characterizes the attenuation to be expected in the building caused by the signal reflections.	1
	Distance [m] between the Tx and the first encountered wall. In this case, it corresponds with the closest wall to the Tx along the direct ray between Tx and Rx. The larger this distance, the less the transmitter antenna is obstructed, leading to a lower expected path loss.	1
	Distance [m] between the Rx and the first encountered wall in the direct ray with the Tx. In this case, it corresponds with the closest wall to the Rx along the direct ray between Tx and Rx. The larger this distance, the less the receiver antenna is obstructed, leading to a lower expected path loss.	1
	Reflection loss of the closest wall to the Tx along the direct ray between Tx and Rx (it depends on the incident angle and the wall material). The larger the reflection loss of the first wall, the more the signal will be attenuated.	1
	Reflection loss of the first wall encountered from Tx to Rx, rotated ±10 degrees. Ten degrees forms a trade-off between a sufficient angular diversity from the direct ray (0°) while still considering the zone along which the main part of the power is usually being propagated.	2
Output	Propagation Path Loss [dB].	1

TABLE 3. Parameter settings and link budget parameters for the network optimization. MCS is the Modulation and Coding Scheme. SNR is the Signal Noise Ratio. Rx is the minimal received power to satisfy the SNR requirement accounting for the given shadowing and fading margins.

Frequency	28 GHz
Bandwidth	400 MHz
EIRP	5 - 40 dBm
Shadowing Margin [50]	6 dB
Fading Margin [50]	9 dB
Thermal noise power at 300K (@400 MHz bandwidth)	-88.5 dBm
TDD duty cycle DL [51]	0.75
TDD duty cycle UL [51]	0.25

	MCS	Modulation	SNR [dB]	Bitrate [Mbps]	Rx [dBm]
	1	BPSK	-1.4	385	-74.9
	2	BPSK	0.5	770	-73.0
	3	BPSK	2.0	960	-71.5
	4	BPSK	3.5	1150	-70.0
	5	BPSK	4.2	1250	-69.3
	6	BPSK	5.5	1350	-68.0
	7	QPSK	3.5	1540	-70.0
	8	QPSK	4.8	1930	-68.7
	9	QPSK	6.5	2310	-67.0
MCS/Modulation/	10	QPSK	7.5	2500	-66.0
SNR/Bitrate/Rx [52]	11	QPSK	8.5	2700	-65.0
	12	16QAM	9.5	3080	-64.0
	13	16QAM	11.5	3850	-62.0
	14	16QAM	12.8	4620	-60.7
	15	16QAM	13.8	5000	-59.7
	16	16QAM	15.5	5390	-58.0
	17	64QAM	14.5	4620	-59.0
	18	64QAM	16.5	5780	-57.0
	19	64QAM	18.5	6390	-55.0
	20	64QAM	19.5	7500	-54.0
	21	64QAM	21	8080	-52.5

provides the required coverage for all the points inside the building. In the end, this coverage percentage is then verified with the RT software.

According to Table 3 the minimum received signal level we require for a network deployment is approximately -75 dBm (these values were calculated considering a 95% shadowing and 99% fading margin of 9 dB and 6 dB respectively [48]). The *EIRP_AP* used for the network optimization is 5dBm to 40 dBm (see Section III-E.4). Hence, the maximum PL (*EIRP_AP_max* − *Rx*, see Table 3 for Rx values) that is to be considered here is 115 dB. Then, to properly account for the MAE, we train and validate the ML model with PL values higher than 115 dB as only these PL links will be relevant in a network planning process: receiver points with a higher PL will be covered by another AP.

1) ML+GA BASED NETWORK PLANNING APPROACH

To find the optimal deployment with a minimal number of 5G APs and still provide the required quality of service, we use the approach of Figure 1, and the link budget parameters from Table 3. The core of the system is a Genetic Algorithm [47]. The inputs are the floor plan and the PL estimation made with the ML algorithm for every possible AP-Rx link. The output of the model is a set of APs, that

2) ELECTROMAGNETIC EXPOSURE

To find the optimal network deployment, the GA accounts for the minimum number of APs considering coverage requirements (according to Table 3) and the minimum electromagnetic field exposure at 28 GHz.

We consider the incident power density S_{Loc} [W/m^2] at a certain location of the floor as a metric for characterizing the exposure caused by all radiating APs (N_AP) in the network [51].

$$S_{Loc} = \sum_{i=1}^{N\_AP} \frac{E_{AP_i}^2}{377} \quad (5)$$

We derive E_{AP_i} [V/m] [31] from the path loss as follows:

$$E_{AP_i} = 10^{\frac{\left(EIRP_{AP_i} + 10 \cdot log_{10}(DC_{TDD}^{DL}) - 43.15 + 20 \cdot log_{10}(f_{AP_i}) - PL\right)}{20}} \quad (6)$$

where PL is the Path Loss in [dB], f_{AP_i} is the AP frequency in [MHz], DC_{TDD}^{DL} is the TDD duty cycle in the downlink ($DC_{TDD}^{DL} = 0.75$) capturing the fact that the BS does not transmit continuously during the data connection. To obtain an optimal network deployment, the GA aims to minimize the s (see Equation (9)).

3) GENETIC ALGORITHM

The GA was modified to find the minimal number of APs, maximum coverage percentage, and minimum exposure, but still providing the required bitrate, according to Table 3. Figure 3 shows the flow graph of the modified GA for finding the minimal number of APs. In the GA, a possible network solution is called *"Individual"*, and it is characterized by an array containing the state of the respective APs, where each AP corresponds to a gene of a solution. Every *Individual* ($X_i, i = 1 \cdots .population\_size$) is represented by an M-dimensional vector, where M is the number of candidate APs (locations are set on a 4 m grid spanning the entire building). Finally, M is equal to 70 for iGent building and 97 for Zuiderpoort building (we refer the reader to Section IV-B).

$$X_i = (X_{i,1}, X_{i,2}, \ldots, X_{i,M}) \quad (7)$$

with $X_{i,j}, j = 1 \cdots M$, a gene of the solution X_i, representing either switched off (set to 0) or switched on (set to 1) [47].

The GA starts with an *"Initialization"* step during which the scenario parameters are set. It defines the minimum Rx signal level (Rx_{Min}) which is equal to the Rx threshold defined in Table 3, the value of incident power density (S_{Area}), which is the current maximal power density when all possible AP candidates are deployed in the building, initially set as $S_{Area_{Max}}$, and the EIRP_AP = 40 dBm (the maximum possible value), which is changing during the optimization process.

To characterize the exposure on a building floor, we use the incident power density in the entire area (S_{Area}) [31] (defined in equation (8)). This metric combines the average $S_{Area_{50}}$ (50 percentile of the S_{Loc} values over the building
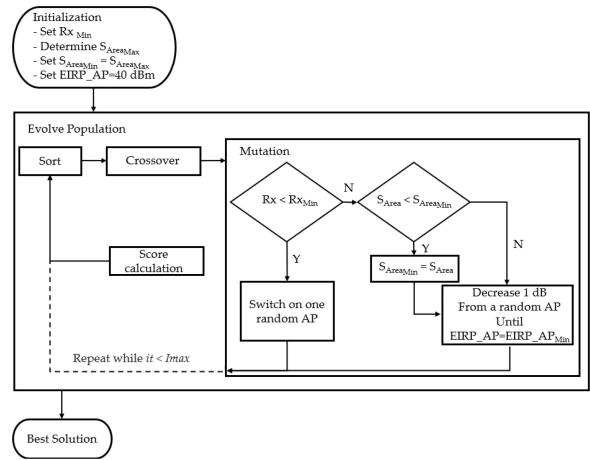
FIGURE 3. Flow graph of Genetic Algorithm used for network deployment. RX is the received signal level. *s* is the incident power density calculated with Equation (9).

floor, median value) and $S_{Area_{95}}$ (95 percentile of the S_{Loc} values over the building floor, 'maximal' value), similar to the approach followed in [30]. To account for the minimum value of S_{Area} ($S_{Area_{Min}}$), in the "Initialization" process we define it as $S_{Area_{Max}}$. In every iteration, the GA calculates a new value of S_{Area} and it is compared with the previously calculated value and should be lower or equal (if true, the $S_{Area_{Min}} = S_{Area}$). After the initialization phase, all candidate APs are randomly switched on (set to 1) or off (set to 0). Each iteration $it(it = 1, \ldots, Imax, Imax = 100)$ consists of the following consecutive steps.

- *Sorting* – sort all previous *"Individuals″* by their score values. The score is based on the solution, where coverage of all grid points is the first requirement, the second one is the minimum number of APs, and the minimal exposure is the last one. To score an individual, we use the following formula:

$$Score = AP_{dep} + (100 - Cov) + K \cdot \frac{S_{Area}}{S_{Area_{Max}}} \quad (8)$$

where AP_{dep} is the sum of the switched-on APs of the solution X_i (see equation (7)), Cov is the percentage of grid points that are covered with the minimum Rx level, S_{Area} is the incident power density value calculated with the equation (9), K is a factor used to balance the weight of each the three criteria in the formula ($K = 5$), and $S_{Area_{Max}}$ is the maximum value of S_{Area} calculated in the "Initialization″ process.

$$S_{Area} = \frac{\left(w_1 \cdot S_{Area_{50}} + w_2 \cdot S_{Area_{95}}\right)}{(w_1 + w_2)} \quad (9)$$

Where $S_{Area_{50}}$ and $S_{Area_{95}}$ are the 50 percentile and 95 percentile respectively of the incident power density values over the considered area. We choose to include $S_{Area_{50}}$ into the metric to account for the median exposure on the building floor, and also $S_{Area_{95}}$, to account for the maximal exposure values. Here, we will

assume an equal impact of $S_{Area_{50}}$ and $S_{Area_{95}}$ on the metric and set both w_1 and w_2 at a value of 0.5 [31].

- *Crossover* – from the sorted population, a new population is created where the *best_individuals* are transferred unchanged to the new population. The other new child solutions (*population_size $\rightarrow$ best_individuals*) are obtained from a crossover operation between two individuals. Each child gene is inherited from either one of the corresponding parent genes, with equal probability. The newly created child solution is added to the new population.

- *Mutation* – It is the process where all the "*Individuals*" in the new solution are mutated. Based on the score, if the new score is lower than the old one, the mutated individual replaces the old population. Otherwise, another "*Individual*" is selected looking for a better score. The mutation operation is as follows:

  - If not all receiver locations are covered ($Rx < Rx_{Min}$), one inactive AP close to the uncovered area is switched on.
  - If all receiver locations are covered ($Rx \geq Rx_{Min}$) and $S_{Area} < S_{Area_{Min}}$, the value of $S_{Area_{Min}}$ is now the new one calculated ($S_{Area_{Min}} = S_{Area}$) and the EIRP of one random AP is decreased 1 dB (or switched off when its power is equal to EIRP_AP$_{Min}$).
  - If all receiver locations are covered ($Rx \geq Rx_{Min}$), but $S_{Area} > S_{Area_{Min}}$ the EIRP of one random AP is decreased 1 dB (or switched off when its power is equal to EIRP_AP$_{Min}$).

4) NETWORK OPTIMIZATION

As the goal for maximizing coverage and minimizing the amount of APs, contradicts with the goal for minimizing exposure, we define network optimality based on the Pareto theorem [52]. It presents a trade-off between the coverage percentage, the required number of APs in the final deployment, and the power density.

Pareto Efficiency: Pareto optimality is a concept of efficiency used in the social sciences, including economics and political science. The Pareto optimal state is defined as a state where it is not possible to make a single objective better without making at least another one worse [53]. In engineering, it is used when more than one parameter needs to be optimized (multi-objective optimization problem). Then, for a set of choices and a metric to value them, it is possible to find a set that is Pareto efficient. This is called the Pareto front (set of non-dominated solutions) [54]. Hence using the Pareto front, it is possible to determine the trade-off between all parameters depending on the design constraints.

In Pareto optimization, the maximization of a certain parameter leads to the minimization of at least one other. Then, it is possible to evaluate several combinations of performance indicators, each one with a certain weight (Pareto coefficient) in the optimization algorithm. The general Pareto equation P is defined as a set of n independent metrics G multiplied by a certain weight W.

$$P(W_1; W_2; \cdots ; W_n)$$
$$= \{W_1 \cdot G_1; W_2 \cdot G_2; \cdots ; W_n \cdot G_n\} \quad (10)$$

where for any combination of $W_1; W_2; \cdots ; W_n$ the following condition should be satisfied:

$$\sum_{i=1}^{n} W_i = 1 \quad (11)$$

Network Optimization: Section III-E.1 describes the procedure to minimize the number of APs and the exposure by means of the incident power density, and maximize the coverage percentage in an indoor environment using a *ML+ GA* approach.

For the network optimization, the algorithm dynamically changes the *EIRP_AP* from 5 to 40 dBm for each candidate solution the GA encounters in the process. For each combination of the Pareto coefficients (coefficients defining how each parameter is weighted when optimizing the network), a network solution is retrieved with different *EIRP_AP* value, different coverage percentage, different exposure value, and returns the number of APs.

The GA will obtain the network deployment for different candidate solutions. For each network solution, the three parameters (coverage percentage, number of APs, exposure) are calculated and stored. After all network deployments are retrieved, the whole Pareto population is mapped. Each point in the graph represents a solution for a certain Pareto weight combination. In this way, it is possible to assess the network performance for each parameter and find the best trade-off (Pareto front).

IV. RESULTS AND DISCUSSION
A. PL ESTIMATION WITH MACHINE LEARNING

In Section III-C and D, the inputs of the datasets used for training and validating, and testing the model were presented. To evaluate the model quality, we trained and validated three variants (see Section III-C). Figure 4, shows a scatter plot with the performance of the ML-estimated values vs. the assumed true values (RT software calculation) for the three variants and for the validation building, where the average of the MAE for the three variants is 2.8 dB.
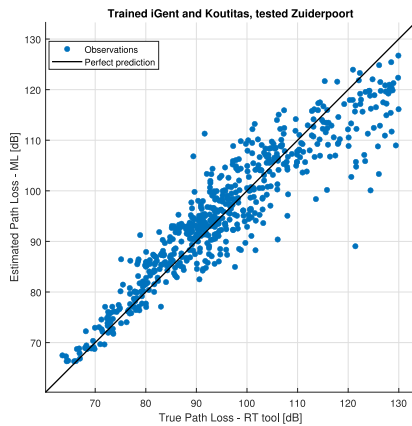
The model trained and validated with iGent and Zuiderpoort buildings and tested with Koutitas building (MAE = 2.5 dB for the maximum allowed PL, Figure 4(a)) performs better than the another two variants (MAE = 2.7 dB, Figure 4(b) and MAE = 3.3 dB, Figure 4(c)). As it has the estimated values closer to the perfect prediction line (black line), especially for low-power APs and high-throughput requirements (i.e., lower path loss links), the obtained MAE values are in line with other models at other frequency bands (i.e., [17], [18], [20]). To validate the MAE in the training process and to make a stable ML PL model, we used the procedure described in Section III-D.1. Figure 5 shows the PAVE of the MAEs value in the training
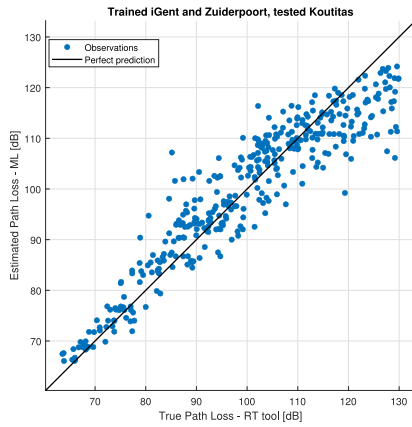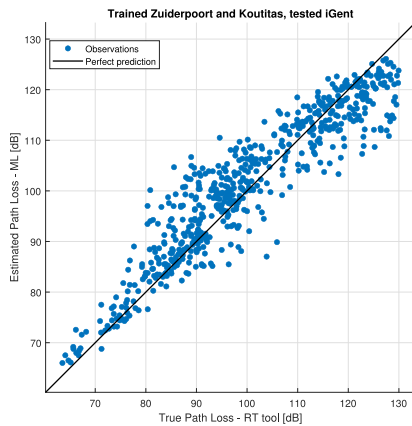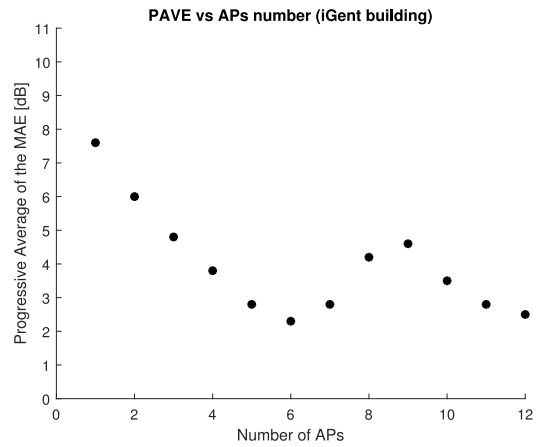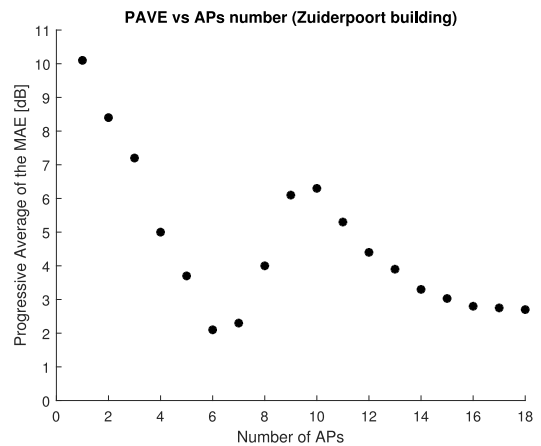
FIGURE 4. PL comparison between the RT software calculation and the ML-estimated ones. (a) Model trained and validated with iGent and Zuiderpoort building and tested with Koutitas building. (b) Model trained and validated with Zuiderpoort and Koutitas building and tested with iGent building. (c) Model trained and validated with iGent and Koutitas building and tested with Zuiderpoort building.
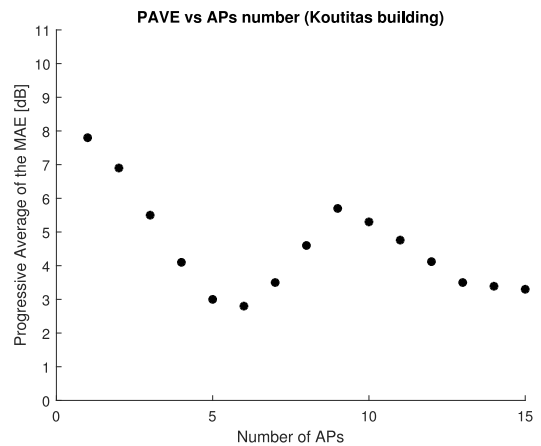

FIGURE 5. Mean Absolute Error validation in the training process, where "Number of APs" is the total number of APs used to build the training and validation dataset. (a) Progressive Average for iGent building. (b) Progressive Average for Zuiderpoort building. (c) Progressive Average for Koutitas building.

process, where the MAE is converging to a value while the number of APs simulated inside the floor is increased. Compared with the results obtained in Section IV-A, using

one building we reduce the MAE, but the generality of the ML model could be reduced.

To illustrate the accuracy of the PL estimations, we compare the received signal power estimated by the proposed ML model with the RT software calculation (*EIRP_AP*=40 dBm) in the building area. Figure 6(c) compares the simulated Rx due to a randomly placed AP, according to the RT software (Figure 6(a)) and according to the ML PL model (Figure 6(b)) for the iGent building. The received signal level was limited to the maximum allowed PL (115 dB, see Table 3). The MAE between the calculation with RT software and the estimation with ML is 3.5 dB.

B. NETWORK PLANNING

1) WIRELESS NETWORK PLANNING

Once we have the ML model trained, validated, and tested, we can now easily adopt the fast and accurate ML model for network planning, using the GA as explained in Section III-E.3. First, we only consider coverage and the number of AP as a constraint (K=0 in Equation (8)). The reception quality specifications for the floors in the three buildings (Section III-C) were taken from Table 3. Figure 7 shows the resulting network deployment based on the setting 12/16QAM/9.5dB/3080 Mbps/−64dBm from Table 3.

Table 4 summarizes the deployment results using the proposed ML+GA, accounting only for the minimum number of APs. The ML model for each scenario is based only on training values collected in the two other buildings, showcasing the envisioned general applicability. The RT software does not include functionality to perform network deployments in an indoor environment, so there is no benchmark to evaluate the quality of the proposed network deployment. However, applying the Wireless InSite software to the ML+GA deployment can assess the coverage percentage of the GA-proposed deployment. Figure 8 shows the network deployment obtained with the combination ML+GA, but in this case, it was assessed using the RT software to compare the coverage requirement. For this network deployment, the MAE between our solution and the calculation made with the RT software is 3.2 dB for iGent building, 3.4 dB for Zuiderpoort building and 2.6 dB for Koutitas building.

Table 4 confirms that the ML+GA-proposed solution is reliable as the coverage percentage with the target throughput is at least 96.6% (1514/1568 receiver points covered). Related to the time to make calculations it can be noticed that the all possible AP candidates, the RT software is more time-consuming (96 minutes for the iGent building, 258 minutes for the Zuiderpoort building, and 110 minutes for Koutitas building) than the ML approach (ML-processing time [min] column in Table 4). It should be pointed out that the points not covered with the aimed throughput are not uncovered: they are covered but possibly with lower throughput. It should be noted, that the ML PL calculation for all possible AP-Rx links for training the model requires a one-time calculation (ML-processing Time

(a)

(b)

(c)
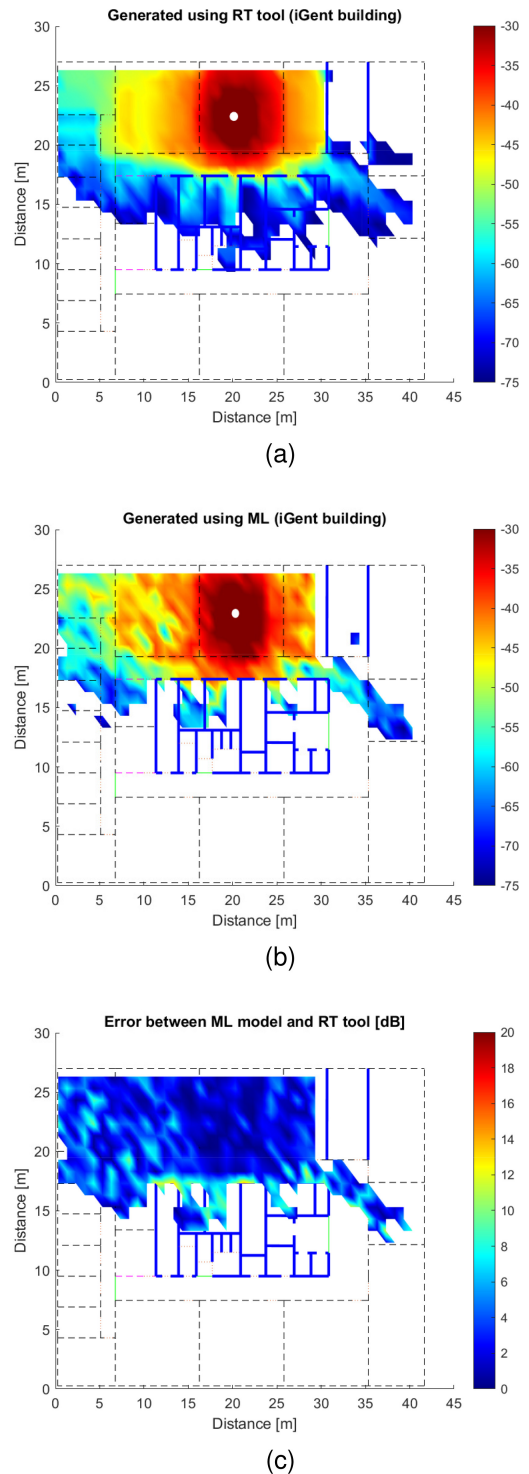
FIGURE 6. Receiver power comparison between the calculation made with Wireless InSite software versus the estimation using the ML model trained and validated with iGent building. White dots are the AP location. *EIRP_AP*= 40 dBm.(a) Estimation with ray-tracing software. (b)Estimation with ML model. (c) Error [dB] between the ML model and the RT software.

in Table 4). However, these values can be re-used when another throughput requirement is set or when room-specific requirements are set.

TABLE 4. Summary of the network deployment using the ML+GA proposal for the setting 12/16QAM/9.5dB/3080 Mbps/-64dBm and accounting only for the minimum number of APs. *EIRP_AP* = 20 dBm. *MAE between the calculation made by the RT software and the estimation made by the ML+GA approach for this network deployment.

Scenario	Possible APs locations	Required APs	RT calculation time [min]	ML-Processing time [min]	GA Optimization time [min]	% Rx Covered ML+GA	% Rx Covered RT tool	S (95 percentile) $[\mu W/m^2]$	MAE* [dB]
iGent	70	15	128	31	0.20	97.2	98	0.428	3.2
Zuiderpoort	97	18	307	104	0.28	96.6	96	0.556	3.4
Koutitas	60	21	135	43	0.22	96.8	97.1	0.415	2.6

TABLE 5. Network deployment using the ML+GA proposal for the setting 12/16QAM/9.5dB/3080Mbps/-64dBm and accounting for minimum Electromagnetic Exposure. *EIRP_AP* = 17 dBm. *MAE between the calculation made by the RT software and the estimation made by the ML+GA approach.

Scenario	Possible APs locations	Required APs	RT calculation time [min]	ML-Processing time [min]	GA Optimization time [min]	% Rx Covered ML+GA	% Rx Covered RT tool	S (95 percentile) $[\mu W/m^2]$	Reduction $[\mu W/m^2]$	MAE* [dB]
iGent	70	20	128	31	0.13	96.5	97.3	0.315	0.113 (26.4%)	2.9
Zuiderpoort	97	23	307	104	0.21	97.3	98	0.435	0.121 (21.7%)	2.5
Koutitas	60	24	135	43	0.25	97.6	98.3	0.319	0.128 (23.1%)	3.4

2) WIRELESS NETWORK PLANNING FOR MINIMUM HUMAN ELECTROMAGNETIC EXPOSURE

To account for the human exposure, we set parameter *K* in Equation (8) to (5). Table 5 summarizes the deployment using the proposal ML+GA accounting for minimum power density. To validate the approach of introducing this constraint, we evaluated the average received power of the GA-proposed deployment, according to the RT software. By comparing the results in terms of coverage percentage, we can notice that the RT tool shows around 1% more than the ML+GA. The results show that S is indeed reduced (at least 21%) after applying the exposure minimization (see column 'Reduction' in Table 5), but at the expense of a higher number of required APs (+3 for the three buildings). However, in the validation with the RT tool the reduction of S is 19%, but at the expense of a higher coverage. These results illustrate the trade-off between the number of APs and the exposure within the network.

Therefore, we investigate this trade-off via the Pareto front shon in Figure 9. Using equation (11) the simulations were performed, and the three parameters (coverage percentage, number of required AP and transmitted power) were stored. In the end, we show five different graphs, which represent the Pareto front for the 95% (the minimum coverage percentage we guarantee in our design) to 100% coverage. For a low number of deployed APs, and different coverage percentage value a different value of S_{Area} was obtained, which means if we need more coverage keeping low the number of AP, the *EIRP_AP* should be higher. However, when the number of APs is increased (corresponding with a lower possible *EIRP_AP*), the S_{Area} value trends to a minimum of 0.02 $\mu W/m^2$ with a more homogeneous exposure value in the area.

3) COMPUTATIONAL COMPLEXITY

The proposed method in this research consists of a GA with a path loss model based on a ML-model, drastically improving calculation time compared to a traditional approach of a GA with a ray-tracing PL model.

The overall computational complexity of an SBR ray tracer, for a single transmitter-receiver link, increases with the number of rays launched by the transmitter, the number of objects to be tested for intersections with the rays. Complexity increases linearly with the number of allowed reflections and exponentially with the number of diffractions, as diffractions involve the creation of new rays around the diffracting edge [55]. Making abstraction of this difference and treating them as similar interactions, we can consider the complexity for one given access point location to be $O(rnm^3)$, with r the number of receiver points in the area, n the number of rays shot per transmitter-receiver link, and m the number of elements in the environment that could interact with each ray (here assuming 3 possible interactions). In the context of network planning, where a lot of different candidate access point locations need to be evaluated, this rapidly leads to excessive calculation time.

The complexity of the (one-time) offline training of the machine learning model is largely determined by the matrix operations involved in handling the covariance matrix K of the data, with dimensions nxn, where the *n* is the number (data from two buildings) of data points used in the dataset ($n = 14391$ for iGent building, $n = 27234$ for Zuiderpoort building and $n = 14400$ for Koutitas building, see Table 1). The complexity for this algorithm is given by $O(n^3)$ [56]. One data point corresponds to a ray tracing calculation for one transmitter-receiver link. Once the machine learning model is obtained, its evaluation is solving a linear equation to obtain the PL corresponding with the set of correlated inputs.
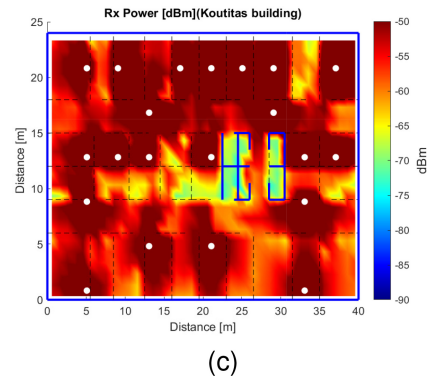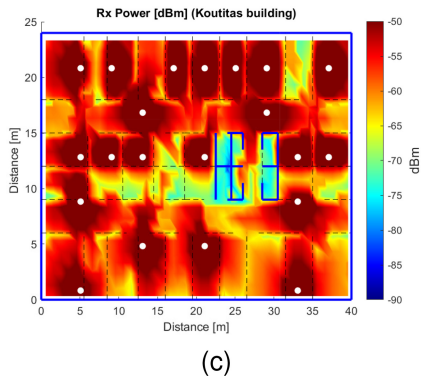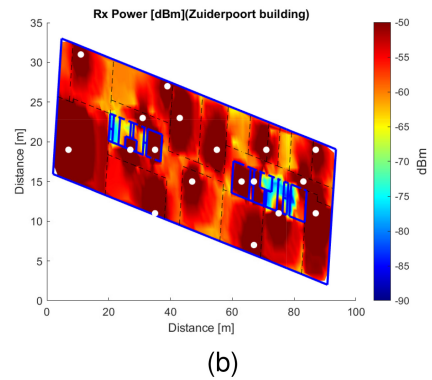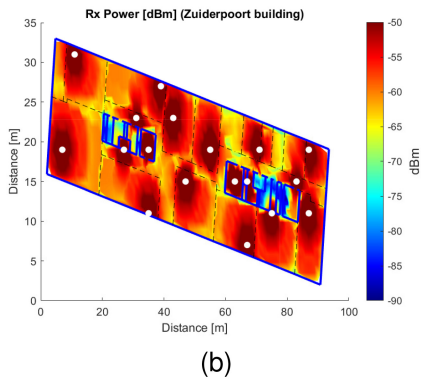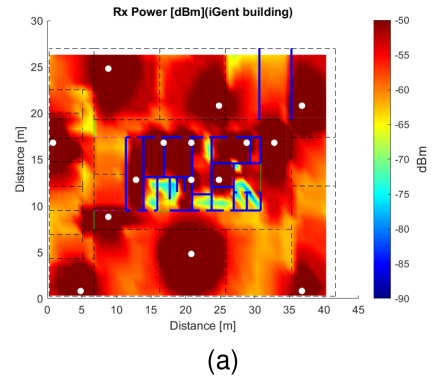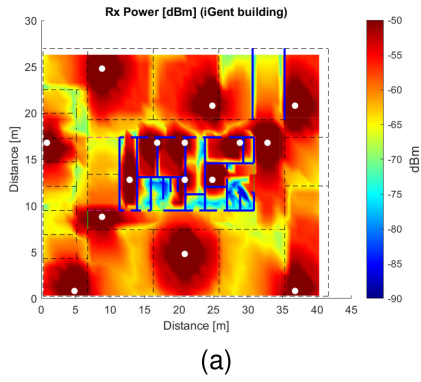
FIGURE 7. Network deployment using GA and ML models for 12/16QAM/9.5dB/3080 Mbps/-64dBm (See Table 3) and accounting only for the minimum number of APs. White dots represent the APs locations. *EIRP_AP* = 20 dBm. (a) iGent building. (b) Zuiderpoort building. (c) Koutitas building.


FIGURE 8. Network deployment tested with ray-tracing software using the APs locations obtained with the combination ML + GA. White dots represent the APs locations. *EIRP_AP* = 20 dBm. (a) iGent building. (b) Zuiderpoort building. (c) Koutitas building.

In general, the computational complexity of GAs depends on various factors and settings. The overall computational complexity of a genetic algorithm per generation can be estimated as the sum of the complexities of evaluating the fitness of all individuals, performing selection, crossover, and mutation. Thus, for one generation, the complexity might be approximated as $C = O(N * C_f + N * C_{GO})$, with N the population size, Cf the complexity of evaluating the fitness function, and C the total complexity of the genetic operations (selection, crossover, mutation). Here, C_f (equation (7)) is a simple linear evaluation. Given G generations, the total complexity of the GA would be, $C = O(G * N * (C_f + C_{GO}))$ [57].

The main advantage of the proposed approach in this research, is that the ML model is trained and validated only once, offering a flexible solution (optimized with a GA) that can quickly optimize deployments with other QoS, energy, and/or exposure constraints. However, using ray tracing in combination with a GA is not feasible when we must evaluate several candidates for network deployments because of the high demand of computational resources and time consuming.

V. CONCLUSION AND FUTURE WORK
We propose a novel indoor 5G network planning approach in the mmWave (28GHz) based on the combination of Machine Learning and a Genetic Algorithm. With information from two buildings, we constructed a generic model (validated
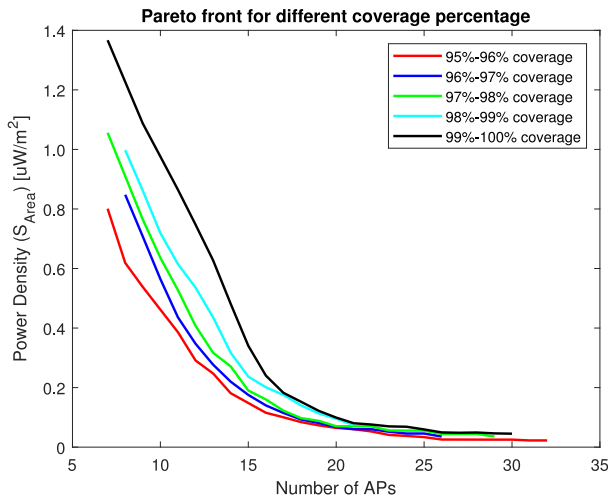
FIGURE 9. Trade-off between the required number of APs and the 95 percentile of S_{Area} varying the transmitted power.

in other building) able to estimate the PL generated by a complex ray-tracing model (Remcom Wireless Insite) based on information related to the floor environment. We use a GP algorithm to build the generic PL model. In the second phase, the ML model is used in combination with a GA to perform network planning for finding the minimal number of APs to provide coverage and accounting for the minimum electromagnetic exposure. The proposed ML+GA is able to provide the desired coverage requirements to at least 95% of the Rx points with an average of the MAE of 4.9 dB (compared to the ray-tracer PL output) and provides full flexibility towards re-planning, with only a minor impact on model performance. Accounting for a minimum of electromagnetic exposure our model was able to reduce the incident power density by at least 18%. A Pareto front showed how network deployments form a trade-off between exposure, the required number of APs, and coverage percentage.

Future work will consist of using the ML+GA approach in combination with massive MIMO and beam-forming to perform exposure-aware network planning in a dynamic industrial scenario with operators performing specific tasks inside a factory (Industry 4.0).

REFERENCES

[1] R. Dangi, P. Lalwani, G. Choudhary, I. You, and G. Pau, "Study and investigation on 5G technology: A systematic review," *Sensors*, vol. 22, no. 1, p. 26, 2021.

[2] U. Ali et al., "Large-scale dataset for the analysis of outdoor-to-indoor propagation for 5G mid-band operational networks," *Data*, vol. 7, no. 3, p. 34, Mar. 2022. [Online]. Available: https://doi.org/10.3390/data7030034

[3] M. Attaran, "The impact of 5G on the evolution of intelligent automation and industry digitization," *J. Ambient Intell. Human. Comput.*, vol. 14, pp. 1–17, Feb. 2021.

[4] M. H. Alsulami, "Challenges facing the implementation of 5G," *J. Ambient Intell. Human. Comput.*, vol. 14, pp. 1–14, Apr. 2022.

[5] N. K. Mallat, M. Ishtiaq, A. Ur Rehman, and A. Iqbal, "Millimeter-wave in the face of 5G communication potential applications," *IETE J. Res.*, vol. 68, no. 4, pp. 2522–2530, 2022.

[6] M. M. Azari et al., "Evolution of non-terrestrial networks from 5G to 6G: A survey," *IEEE Commun. Surveys Tuts.*, vol. 24, no. 4, pp. 2633–2672, 4th Quart., 2022.

[7] T. T. Oladimeji, P. Kumar, and M. K. Elmezughi, "Path loss measurements and model analysis in an indoor corridor environment at 28 GHz and 38 GHz," *Sensors*, vol. 22, no. 19, p. 7642, 2022.

[8] M. Kohli et al., "Outdoor-to-indoor 28 GHz wireless measurements in manhattan: Path loss, location impacts, and 90% coverage," in *Proc. 23rd Int. Symp. Theory, Algorithm. Found., Protocol Design Mobile Netw. Mobile Comput.*, 2022, pp. 201–210.

[9] U. Ullah, U. R. Kamboh, F. Hossain, and M. Danish, "Outdoor-to-indoor and indoor-to-indoor propagation path loss modeling using smart 3D ray tracing algorithm at 28 GHz mmWave," *Arab. J. Sci. Eng.*, vol. 45, no. 12, pp. 10223–10232, Dec. 2020. [Online]. Available: https://doi.org/10.1007/s13369-020-04661-w

[10] D. Plets, W. Joseph, K. Vanhecke, E. Tanghe, and L. Martens, "Coverage prediction and optimization algorithms for indoor environments," *EURASIP J. Wireless Commun. Netw.*, vol. 2012, no. 1, pp. 1–23, Mar. 2012.

[11] E. Ozturk, F. Erden, K. Du, C. K. Anjinappa, O. Ozdemir, and I. Guvenc, "Ray tracing analysis of sub-6 GHz and mmWave indoor coverage with reflecting surfaces," in *Proc. IEEE Radio Wireless Symp. (RWS)*, 2022, pp. 160–163.

[12] O. A. Topal, M. Ozger, D. Schupke, E. Björnson, and C. Cavdar, "mmWave communications for indoor dense spaces: Ray-tracing based channel Characterization and performance comparison," 2022, *arXiv:2202.08774*.

[13] M. Lecci et al., "Simplified ray tracing for the millimeter wave channel: A performance evaluation," in *Proc. Inf. Theory Appl. Workshop (ITA)*, 2020, pp. 1–6.

[14] D. He, B. Ai, K. Guan, L. Wang, Z. Zhong, and T. Kürner, "The design and applications of high-performance ray-tracing simulation platform for 5G and beyond wireless communications: A tutorial," *IEEE Commun. Surveys Tuts.*, vol. 21, no. 1, pp. 10–27, 1st Quart., 2018.

[15] M. U. Sheikh, F. Ghavimi, K. Ruttik, and R. Jantti, "Analysis of indoor solutions for provision of indoor coverage at 3.5 GHz and 28 GHz for 5G system," in *Proc. 26th Int. Conf. Telecommun. (ICT)*, 2019, pp. 340–345. [Online]. Available: http://dx.doi.org/10.1109/ICT.2019.8798826

[16] W. Zhu, C.-L. Huang, W.-C. Yeh, Y. Jiang, and S.-Y. Tan, "A novel bi-tuning SSO algorithm for Optimizing the budget-limited sensing coverage problem in wireless sensor networks," *Appl. Sci.*, vol. 11, no. 21, 2021, Art. no. 10197. [Online]. Available: https://doi.org/10.3390/app112110197

[17] N. Raj, "Indoor RSSI prediction using machine learning for wireless networks," in *Proc. Int. Conf. Commun. Syst. NETworkS (COMSNETS)*, 2021, pp. 372–374.

[18] S. Ma, H. Cheng, and H. Lee, "A practical approach to indoor path loss modeling based on deep learning," *J. Comput. Sci. Eng.*, vol. 15, no. 2, pp. 84–95, 2021.

[19] P. Wang and H. Lee, "Indoor path loss modeling for 5G communications in smart factory scenarios based on Meta-learning," in *Proc. 12th Int. Conf. Ubiquitous Future Netw. (ICUFN)*, 2021, pp. 438–443.

[20] M. E. Diago-Mosquera, A. Aragón-Zavala, and M. Rodriguez, "Towards practical path loss predictions in indoor corridors considering 5G mmWave three-dimensional measurements," *IEEE Antennas Wireless Propag. Lett.*, vol. 21, pp. 2055–2059, 2022.

[21] S. A. Aldossari, "Predicting path loss of an indoor environment using artificial intelligence in the 28-GHz band," *Electronics*, vol. 12, no. 3, p. 497, 2023. [Online]. Available: https://www.mdpi.com/2079-9292/12/3/497

[22] S. Sun et al., "Propagation path loss models for 5G urban micro- and macro-cellular scenarios," in *Proc. IEEE 83rd Veh. Technol. Conf. (VTC)*, 2016, pp. 1–6.

[23] A. J. Flórez-González, C. A. Viteri-Mera, and W. O. Achicanoy-Martínez, "Fast indoor radio propagation prediction using deep learning," in *Proc. 18th Eur. Conf. Antennas Propag. (EuCAP)*, 2024, pp. 1–6. [Online]. Available: http://dx.doi.org/10.23919/EuCAP60739.2024.10500989

[24] B. Batista Nascimento Silva and E. T. C.Santos, "A python tool to predict wireless network signals in indoor environments using neural networks," *Set Int. J. Broadcast Eng.*, vol. 2023, no. 1, Dec. 2023. [Online]. Available: http://dx.doi.org/10.18580/setijbe.2023.4

[25] T. K. Geok et al., "3D RT adaptive path sensing method: RSSI modelling validation at 4.5 GHz, 28 GHz, and 38 GHz," *Alex. Eng. J.*, vol. 61, no. 12, pp. 11041–11061, Dec. 2022. [Online]. Available: https://doi.org/10.1016/j.aej.2022.04.033

[26] F. Hossain et al., "An efficient 3-D ray tracing method: Prediction of indoor radio propagation at 28 GHz in 5G network," *Electronics*, vol. 8, no. 3, p. 286, 2019. [Online]. Available: https://www.mdpi.com/2079-9292/8/3/286

[27] Z. Yun and M. F. Iskander, "Ray tracing for radio propagation modeling: Principles and applications," *IEEE Access*, vol. 3, pp. 1089–1100, 2015.

[28] *IEEE Standard For Safety Levels With Respect to Human Exposure to Radio Frequency Electromagnetic Fields*, 3 kHz to 300 GHz, IEEE Standard C95.1, 1999, pp. 1–83.

[29] International Commission Non-Ionizing Radiation Protection, "Guidelines for limiting exposure to time-varying electric, magnetic, and electromagnetic fields (up to 300 GHz)," *Health Phys.*, vol. 74, no. 4, pp. 494–522, 1998.

[30] D. Plets, W. Joseph, K. Vanhecke, and L. Martens, "Exposure optimization in indoor wireless networks by heuristic network planning," *Prog. Electromagn. Res.*, vol. 139, pp. 445–478, May 2013.

[31] D. Plets et al., "Joint minimization of uplink and downlink whole-body exposure dose in indoor wireless networks," *BioMed Res. Int.*, vol. 2015, Feb. 2015, Art. no. 943415.

[32] G. Castellanos et al., "Multi-objective optimisation of human exposure for various 5G network topologies in Switzerland," *Comput. Netw.*, vol. 216, Oct. 2022, Art. no. 109255. [Online]. Available: https://doi.org/10.1016/j.comnet.2022.109255

[33] A. W. Reza, M. Sarker, and K. Dimyati, "A novel integrated mathematical approach of ray-tracing and genetic algorithm for Optimizing indoor wireless coverage," *Prog. Electromagn. Res.*, vol. 110, pp. 147–162, Jan. 2010.

[34] S. Xing, "Research on indoor wireless network coverage layout based on hybrid particle swarm optimization algorithm," in *Proc. IEEE 3rd Int. Conf. Electron. Technol., Commun. Inf. (ICETCI)*, 2023, pp. 1116–1119. [Online]. Available: http://dx.doi.org/10.1109/ICETCI57876.2023.10176947

[35] R. Kawecki, S. Hausman, and P. Korbel, "Performance of fingerprinting-based indoor positioning with measured and simulated RSSI reference maps," *Remote Sens.*, vol. 14, no. 9, p. 1992, 2022. [Online]. Available: https://www.mdpi.com/2072-4292/14/9/1992

[36] A. Taha, M. Alrabeiah, and A. Alkhateeb, "Enabling large intelligent surfaces with compressive sensing and deep learning," *IEEE Access*, vol. 9, pp. 44304–44321, 2021.

[37] D. Rubinstein, I. Georgiev, B. Schug, and P. Slusallek, "RTSG: Ray tracing for X3D via a flexible rendering framework," in *Proc. 14th Int. Conf. 3D Web Technol.*, 2009, pp. 43–50. [Online]. Available: https://doi.org/10.1145/1559764.1559771

[38] E. Schulz, M. Speekenbrink, and A. Krause, "A tutorial on Gaussian process regression: Modelling, exploring, and exploiting functions," *J. Math. Psychol.*, vol. 85, pp. 1–16, Aug. 2018. [Online]. Available: https://www.sciencedirect.com/science/article/pii/S0022249617302158

[39] J. Quinonero-Candela and C. E. Rasmussen, "A unifying view of sparse approximate Gaussian process regression," *J. Mach. Learn. Res.*, vol. 6, pp. 1939–1959, Dec. 2005.

[40] J. Melo, "Gaussian processes for regression: A tutorial," Dept. Electr. Comput. Eng., University of Porto, Porto, Portugal, Rep. 201201, 2012.

[41] D. Gammelli, K. P. Rolsted, D. Pacino, and F. Rodrigues, "Generalized multi-output Gaussian process censored regression," *Pattern Recognit.*, vol. 129, Sep. 2022, Art. no. 108751.

[42] C. K. I. Williams, *Prediction with Gaussian Processes: From Linear Regression to Linear Prediction and Beyond*. Dordrecht, The Netherlands: Springer, 1998, pp. 599–621. [Online]. Available: http://dx.doi.org/10.1007/978-94-011-5014-9_23

[43] G. Koutitas and T. Samaras, "Exposure minimization in indoor wireless networks," *IEEE Antennas Wireless Propag. Lett.*, vol. 9, pp. 199–202, 2010. [Online]. Available: https://doi.org/10.1109/lawp.2010.2045870

[44] *Propagation Data and Prediction Methods for the Planning of Short-Range Outdoor Radiocommunication Systems and Radio Local Area Networks in the Frequency Range 300 MHz to 100 GHz*, ITU-Rec. P. 1411, Int. Telecommun. Union, Geneva, Switzerland, 2023.

[45] C. R. Simovski, "Application of the fresnel formulas for reflection and transmission of electromagnetic waves beyond the quasi-static approximation," *J. Commun. Technol. Electron.*, vol. 52, no. 9, pp. 953–971, Sep. 2007. [Online]. Available: http://dx.doi.org/10.1134/S1064226907090021

[46] T. Mahmood, H. K. Al-Qaysi, and A. S. Hameed, "The effect of antenna height on the performance of the Okumura/Hata model under different environments propagation," in *Proc. Int. Conf. Intell. Technol. (CONIT)*, 2021, pp. 1–4.

[47] Y. Hervis Santana, R. Martinez Alonso, G. Guillen Nieto, L. Martens, W. Joseph, and D. Plets, "Indoor genetic algorithm-based 5G network planning using a machine learning model for path loss estimation," *Appl. Sci.*, vol. 12, no. 8, p. 3923, 2022. [Online]. Available: https://www.mdpi.com/2076-3417/12/8/3923

[48] G. R. Maccartney, T. S. Rappaport, S. Sun, and S. Deng, "Indoor office Wideband Millimeter-wave propagation measurements and channel models at 28 and 73 GHz for ultra-dense 5G wireless networks," *IEEE Access*, vol. 3, pp. 2388–2424, 2015.

[49] M. Matalatala et al., "Multi-objective optimization of massive MIMO 5G wireless networks towards power consumption, uplink and downlink exposure," *Appl. Sci.*, vol. 9, no. 22, p. 4974, 2019.

[50] G. Castellanos, B. De Beelde, D. Plets, L. Martens, W. Joseph, and M. Deruyck, "Evaluating 60 GHz FWA deployments for urban and rural environments in Belgium," *Sensors*, vol. 23, no. 3, p. 1056, 2023. [Online]. Available: https://www.mdpi.com/1424-8220/23/3/1056

[51] R. Wydaeghe et al., "Realistic human exposure at 3.5 GHz and 28 GHz for distributed and collocated MaMIMO in indoor environments using hybrid ray-tracing and FDTD," *IEEE Access*, vol. 10, pp. 130996–131004, 2022.

[52] R. M. Alonso, D. Plets, M. Deruyck, L. Martens, G. G. Nieto, and W. Joseph, "Multi-objective optimization of cognitive radio networks," *Comput. Netw.*, vol. 184, Jan. 2021, Art. no. 107651.

[53] T. H. B. Huy, P. Nallagownden, K. H. Truong, R. Kannan, D. N. Vo, and N. Ho, "Multi-objective search group algorithm for engineering design problems," *Appl. Soft Comput.*, vol. 126, Sep. 2022, Art. no. 109287. [Online]. Available: https://www.sciencedirect.com/science/article/pii/S1568494622004811

[54] Y. Hua, Q. Liu, K. Hao, and Y. Jin, "A survey of evolutionary algorithms for multi-objective optimization problems with irregular Pareto fronts," *IEEE/CAA J. Automatica Sinica*, vol. 8, no. 2, pp. 303–318, Feb. 2021.

[55] Z. Yun and M. F. Iskander, "Radio propagation modeling and simulation using ray tracing," in *The Advancing World of Applied Electromagnetics In Honor and Appreciation of Magdy Fahmy Iskander*. Cham, Switzerland: Springer, 2024, pp. 251–279.

[56] J. Wang, "An intuitive tutorial to Gaussian process regression," *Comput. Sci. Eng.*, vol. 25, no. 4, pp. 4–11, Jul. 2023. [Online]. Available: http://dx.doi.org/10.1109/MCSE.2023.3342149

[57] A. Lissovoi and P. S. Oliveto, "Computational complexity analysis of genetic programming," in *Theory of Evolutionary Computation*. Cham, Switzerland: Springer, 2019.

YOSVANY HERVIS SANTANA was born in Matanzas, Cuba, in 1988. He received the B.Sc. degree in telecommunications and electronics engineering and the M.Sc. degree in digital systems from the Higher Polytechnic Institute CUJAE, Havana, Cuba, in 2012 and 2017, respectively. He is currently pursuing the Ph.D. degree with the WAVES Group, Department of Information Technology, Ghent University. Since 2012, he is a Fellow Researcher with LACETEL. He also has collaborated on DTV Engineering Projects with KitKing and Konka, China.

RODNEY MARTINEZ ALONSO (Senior Member, IEEE) received the B.Sc. degree in telecommunications and electronics engineering and the M.Sc. degree in digital systems from Havana University of Technology (CUJAE) in 2010 and 2015, respectively, and the Ph.D. degree in electrical engineering from Ghent University in June 2020. He worked as a Research Engineer with LACETEL, Research and Development Telecommunications Institute from 2010 to 2021. In 2016, he joined WAVES Group (Department of Information Technology—INTEC, Ghent University), where his main research was focused on dynamic spectrum access technologies. He is currently a Senior Researcher with the Department of Electrical Engineering, KU Leuven, with his main research interest in artificial intelligence applications for next generation wireless networks.

GLAUCO GUILLEN NIETO (Senior Member, IEEE) was born in 1961 in Havana, Cuba. He received the B.Sc. degree in radiocommunications and broadcasting engineering and the Ph.D. degree from the Odessa National Academy of Telecommunication (Formerly, Electrotechnical Institute of Communication "A. S. Popov"), Ukraine, in 1985 and 1989, respectively. He has been currently a Senior Researcher with the Research and Development Telecommunications Institute, LACETEL, Academician of Merit of the Cuban Academy of Sciences and a member since 2012. He has been an Adviser of National Network Operator. He also has collaborated in different projects with Finline Technology, Canada; DTV National Engineering Lab (DTVNEL), Beijing; and HAIER and KONKA, China. His current research interests are digital TV broadcasting and wireless communication systems.

LUC MARTENS (Member, IEEE) received the M.Sc. degree in electrical engineering from Ghent University, Belgium, in July 1986, and the Ph.D. degree in December 1990. From September 1986 to December 1990, he was a Research Assistant with the Department of Information Technology (INTEC), Ghent University. During this period, his scientific work was focused on the physical aspects of hyperthermic cancer therapy. His research work dealt with electromagnetic and thermal modeling and with the development of measurement systems for that application. Since 1991, he manages the Wireless and Cable Research Group, INTEC. Since April 1993, he has been a Professor with Ghent University. He is currently a member of IMEC—WAVES Group (Department of Information Technology—INTEC, Ghent University). His experience and current interests are in modeling and measurement of electromagnetic channels, of electromagnetic exposure, e.g., around telecommunication networks and systems, such as cellular base station antennas, and of energy consumption in wireless networks. He is author or coauthor of more than 300 publications in the domain of electromagnetic channel predictions, dosimetry, exposure systems, and health and wireless communications.

WOUT JOSEPH (Senior Member, IEEE) was born in Ostend, Belgium, in October 1977. He received the M.Sc. degree in electrical engineering from Ghent University, Belgium, in July 2000 and the Ph.D. degree in March 2005. This work dealt with measuring and modeling of electromagnetic fields around base stations for mobile communications related to the health effects of the exposure to electromagnetic radiation. He was a Postdoctoral Fellow with FWO-V Research Foundation, Flanders, from 2007 to 2012 . Since October 2009, he is Professor with the domain of "Experimental Characterization of Wireless Communication Systems." He is IMEC PI since 2017. His professional interests are electromagnetic field exposure assessment, propagation for wireless communication systems, and antennas and calibration. Furthermore, he specializes in wireless performance analysis and quality of experience.

DAVID PLETS (Member, IEEE) was born in Belgium, in 1983. He received the master's and Ph.D. degrees in 2006 and 2011, respectively. He is currently a member of IMEC, WAVES Group, Department of Information Technology, Ghent University. His current research interests include low-exposure wireless indoor network planning, cognitive networks, WiFi QoS optimization, and localization algorithms.